

IEICE Proceeding Series

Asynchronous cellular automaton model of spiral ganglion cell and its parallel spike coding

Masato IZAWA, Hiroyuki TORIKAI

Vol. 2 pp. 256-259

Publication Date: 2014/03/18

Online ISSN: 2188-5079

Downloaded from www.proceeding.ieice.org

Asynchronous cellular automaton model of spiral ganglion cell and its parallel spike coding

Masato IZAWA[†] and Hiroyuki TORIKAI[‡]

[†]Department of Systems Innovation, Graduate School of Engineering Science, Osaka University,
 1-3, Machikaneyama-cho, Toyonaka, Osaka 560-8531, Japan

[‡]Department of Computer Science, Faculty of Computer Science and Engineering, Kyoto Sangyo University
 Motoyama, Kamigamo, Kita-Ku, Kyoto-City 603-8555, Japan
 Email: izawa@hopf.sys.es.osaka-u.ac.jp, torikai@cse.kyoto-su.ac.jp

Abstract—In this paper, a novel spiral ganglion cell model using an asynchronous cellular automaton is presented. It is shown that the model can reproduce a parallel spike coding function and nonlinear characteristics such as adaptation property of the mammalian cochlear.

1. Introduction

The mammalian ear is divided into the outer ear receiving a sound wave, the middle ear amplifying the sound wave, and the inner ear processing the sound wave. Fig. 1 shows a sketch of the cochlear in a mammalian inner ear. In the cochlear, firstly, the basilar membrane vibrates in response to the sound wave, secondly, the inner hair cell transforms the mechanical vibration into an electrical potential, and thirdly, the spiral ganglion cells encode the electrical potential into paralleled spike-trains. The cochlear of the inner ear has many nonlinearities such as adaptation property of spike density and nonlinear band-pass characteristics [1], [2]. The purpose of this paper is to design a spiral ganglion cell model which has the parallel spike coding function and the adaptation property. First, we present a novel spiral ganglion cell model based on an asynchronous cellular automaton neuron model [3] and an analog chaotic spiking neuron [4]. Second, it is shown by numerical simulations that the model can reproduce the parallel spike coding function and the adaptation property.

2. Presented model

In this section, we present an asynchronous cellular automaton model of spiral ganglion cell. As shown in Fig. 2, this model has the following four resistors whose bit lengths are denoted by positive integers M , L , J , and K , respectively. (1) A recovery resistor is an M -bit shift resistor having an integer state $P \in \mathbb{Z}_M \equiv \{0, 1, \dots, M-1\}$, $M \geq 2$, encoded by the one-hot coding manner, and “ \equiv ” denotes the “definition” hereafter. From a neuron model point of view, the state P can be regarded as recovery valuable. (2) The i th ($i = 0, \dots, N-1$) membrane resistor is an L -bit shift resistor having an integer state $X_i \in \mathbb{Z}_L \equiv \{0, 1, \dots, L-1\}$, $L \geq 2$, encoded by the one-hot coding

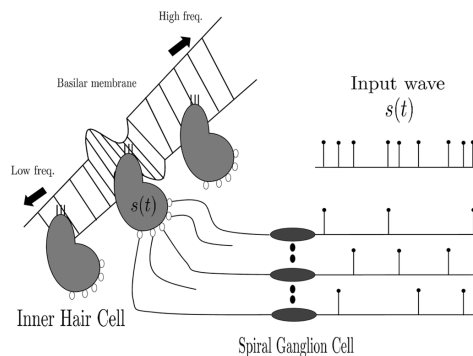


Figure 1: Basic mechanisms of the mammalian inner ear.

manner. From a neuron model point of view, the state X_i can be regarded as membrane potential. (3) A recovery threshold resistor is an J -bit shift resistor having an integer state $Q \in \mathbb{Z}_J \equiv \{0, 1, \dots, J-1\}$, $J \geq 2$, encoded by the one-hot coding manner. The state Q controls a threshold value of the recovery valuable P by making the state Q upward and downward. (4) The i th membrane threshold resistor is an K -bit shift resistor having an integer state $R_i \in \mathbb{Z}_K \equiv \{0, 1, \dots, K-1\}$, $K \geq 2$, encoded by the one-hot coding manner. The state R_i controls a threshold value of the membrane potential X_i by making the state R_i upward and downward. The recovery threshold resistor and the i th membrane threshold resistor realize the adaptation characteristics. The states P , X_i , Q , and R are clamped to the ranges $[0, \dots, M-1]$, $[0, \dots, L-1]$, $[0, \dots, J-1]$, and $[0, \dots, K-1]$, respectively. As shown in Fig. 2, the resistors are connected to each other via the following three memoryless units. (i) The recovery threshold unit consists of logic gates and reconfigurable wires. This unit determines characteristics of the recovery resistor threshold value. (ii) The membrane threshold unit consists of logic gates and reconfigurable wires. This unit determines characteristics of the membrane resistor threshold value. (iii) The reset value unit consists of logic gates and reconfigurable wires. From a neuron model point of view, this unit determines values to which the states P and X_i are reset when one of the val-

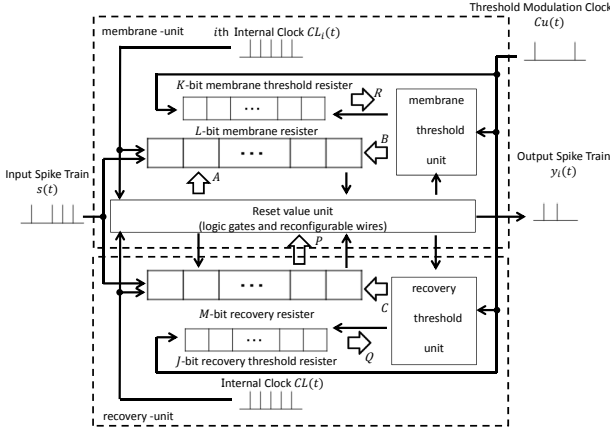


Figure 2: An asynchronous cellular automaton model of spiral ganglion cell.

ues reaches a threshold value. Let t be a continuous time ($t \in [0, \infty)$). The presented model accepts the following three internal clocks: $CL(t)$, $CL_i(t)$, and $Cu(t)$.

$$CL(t) = \begin{cases} 1 & \text{if } t = 1, 2, \dots, \\ 0 & \text{otherwise.} \end{cases}$$

The recovery resistor accepts this clock $CL(t)$. The clock $CL(t)$ has a normalized period 1.

$$CL_i(t) = \begin{cases} 1 & \text{if } t = 1 + \theta_i, 2 + \theta_i, \dots, \quad 0 < \theta_i < 1, \\ 0 & \text{otherwise.} \end{cases}$$

The membrane resistor accepts this clock $CL_i(t)$.

$$Cu(t) = \begin{cases} 1 & \text{if } t = 0, d, \dots, \\ 0 & \text{otherwise.} \end{cases}$$

The recovery valuable threshold and membrane threshold resistors accept this clock $Cu(t)$.

2.1. Autonomous behaviors

Let us explain dynamics of the model. We define the following functions B , C , and A .

$$B(R_i) \equiv \begin{cases} \alpha R_i + \beta, & \text{if } \alpha R_i + \beta \leq L - 1, \\ L - 1, & \text{if } \alpha R_i + \beta > L - 1, \end{cases}$$

$$C(Q) \equiv \begin{cases} \mu Q + \lambda, & \text{if } \mu Q + \lambda \leq M - 1, \\ M - 1, & \text{if } \mu Q + \lambda > M - 1, \end{cases}$$

$$A(P) \equiv C(Q) - 1 - P,$$

$$B : \mathbb{Z}_K \rightarrow \mathbb{Z}_L, \quad C : \mathbb{Z}_J \rightarrow \mathbb{Z}_M, \quad A : \mathbb{Z}_M \rightarrow \mathbb{Z}_L,$$

where $(\alpha, \mu, \beta, \lambda)$ are parameters that characterize threshold values of the model. The parameters (α, μ) determine nonlinearity of the model. The parameters (β, λ) determine minimum threshold values of the state P and the state

X_i . We refer to these functions A , B , and C as the *wiring pattern*.

The transitions of the states $P(t)$, $X_i(t)$, $Q(t)$, and $R_i(t)$ are described by

$$P(t_+) = \begin{cases} P(t) + 1, & \text{if } CL(t) = 1, \\ 0, & \text{if } P(t) \geq C(Q(t)), \quad CL(t) = 1, \\ P(t), & \text{otherwise,} \end{cases}$$

$$X_i(t_+) = \begin{cases} X_i(t) + 1, & \text{if } CL_i(t) = 1, \\ A(P(t)), & \text{if } X_i(t) \geq B(R_i(t)), \quad CL_i(t) = 1, \\ X_i(t), & \text{otherwise,} \end{cases}$$

$$Q(t_+) = \begin{cases} Q(t) - 1, & \text{if } Cu(t) = 1, \quad Q(t) > 0, \\ Q(t) + 1, & \text{if } P(t) \geq C(Q(t)), \quad Q(t) < J - 1, \\ Q(t), & \text{otherwise,} \end{cases}$$

$$R_i(t_+) = \begin{cases} R_i(t) - 1, & \text{if } Cu(t) = 1, \quad R_i(t) > 0, \\ R_i(t) + 1, & \text{if } X_i(t) \geq B(R_i(t)), \quad R_i(t) < J - 1, \\ R_i(t), & \text{otherwise,} \end{cases}$$

where $t_+ = \lim_{\epsilon \rightarrow 0} t + \epsilon$, $\epsilon > 0$. Note that these equations represent the discrete state transitions and thus are implemented by logic gates and reconfigurable wires. In these four equations, if the state $X_i(t)$ reaches the threshold state $B(R_i(t))$, the state $X_i(t)$ is reset to the state $A(P(t))$ controlled by the state $P(t)$, and the model outputs the following spike.

$$y_i(t) = \begin{cases} 1 & \text{if } X_i(t) \geq B(R_i(t)), \\ 0 & \text{otherwise.} \end{cases}$$

Then, we explain each resistors' transitions of the model. The transitions of the state $P(t)$, the state $X_i(t)$, the state $Q(t)$, and the state $R_i(t)$ are described by a cellular automaton. Repeating such integrate-and-fire dynamics, the model outputs a spike-train $y_i(t)$. This output spike-train $y_i(t)$ realizes a property of spike encoding function.

2.2. Non-autonomous behaviors

In this section, we define an input signal of the model. Form a neuron model point of view, the input signal can be regarded as a *stimulation input*.

In a mammalian inner ear, a cochlear accepts a sinusoidal wave as an input signal. So, in this paper, let us apply a Pulse Density Modulation (PDM) of a sinusoidal wave as the input signal of the model. An input signal $s(t)$ is written by

$$s(t) = \begin{cases} 1 & \text{if } t = t_1, t_2, \dots, \\ 0 & \text{otherwise,} \end{cases}$$

where $t = t_1, t_2, \dots$ are an input spike position. The input spike-train $s(t)$ induces the transition of the state $X_i(t)$ and the state $P(t)$ as follows.

$$\begin{aligned} X_i(t_+) &= X_i(t) + s(t), & \text{if } s(t) = 1, \\ P(t_+) &= P(t) + s(t), & \text{if } s(t) = 1. \end{aligned}$$

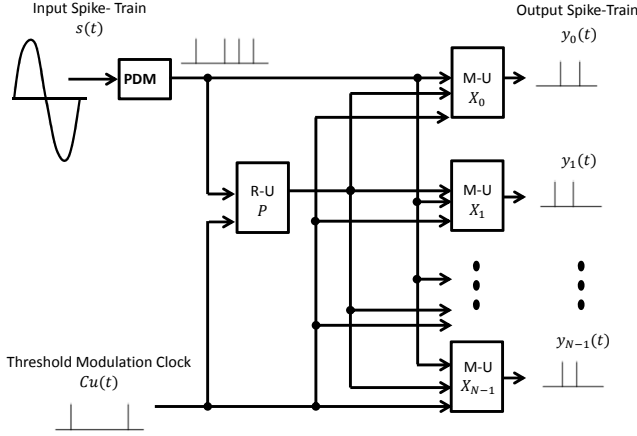


Figure 3: Whole system consists of paralleled N asynchronous cellular automaton model of spiral ganglion cells. An M-U denotes the membrane-unit. An R-U denotes the recovery-unit.

Note again that these equations represent the discrete state transitions and thus are implemented by logic gates and re-configurable wires.

As shown in Fig. 3, the whole system consists of paralleled N asynchronous cellular automaton model of spiral ganglion cells. The membrane resistor and the membrane threshold resistor form the i th membrane-unit, and the recovery resistor and the recovery threshold resistor form a recovery-unit. The input sinusoidal wave $s_{mod}(t)$ is modulated to the input spike-train $s(t)$ by the PDM. Each i th membrane-units and the recovery-unit accept the input spike-train. Each i th membrane-units are connected to the recovery-unit parallelly. In order to analyze the spike coding function, the following logical sum of the spike-trains $\{y_0(t), y_1(t), \dots, y_{N-1}(t)\}$ is introduced.

$$y(t) = \bigcup_{i=0}^{N-1} y_i(t).$$

The model is characterized by the following parameters.

$$N, M, L, J, K, \alpha, \mu, \beta, \lambda.$$

3. Characteristics of presented model

The spiral ganglion cells in the mammalian cochlear have the characteristics of the parallel spike coding function and the adaptation. In this section, we show the two properties are realized by the presented model.

Let us focus on the following parameter values.

$$(N, M, L, J, K, \alpha, \mu, \beta, \lambda) = (20, 288, 192, 64, 64, 3, 2, 96, 64).$$

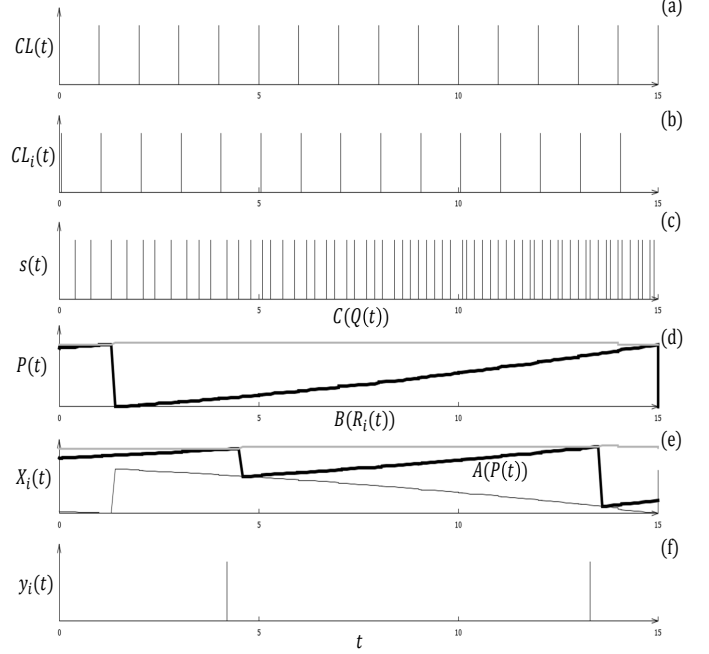


Figure 4: (a) The p -unit's Internal clock $CL(t)$. (b) The x_i -unit's Internal clock $CL_i(t)$. (c) An input signal $s(t)$. (d) The p -unit's internal states. (e) The x_i -unit's internal states. (f) The x_i -unit output spike-train.

In this paper, all the simulations are executed under these parameter values. Note that $N = 20$ is about the same number of human spiral ganglion cells connected to an inner hair cell [1]. Also following [4], we set

$$L = \frac{3}{2}M.$$

3.1. Parallel spike coding function

Fig. 4(d) shows a behavior of the recovery-unit. As shown in this figure, the function $C(Q(t))$ is a threshold value of the state $P(t)$. When the state $P(t)$ reaches the threshold $C(Q(t))$, and the recovery-unit accepts the signal from the internal clock $CL(t)$ or the stimulation input $s(t)$, the state $P(t)$ resets to $P(t) = 0$ and the model outputs a signal to the recovery threshold resistor. Depending on the output signal, the threshold $C(Q(t))$ increases. Repeating this dynamics, the threshold value of the state $P(t)$ increases. Fig. 4(e) shows a behavior of the i th membrane-unit. As shown in this figure, the function $B(R_i(t))$ is a threshold value of the state $X_i(t)$, and the $A(P(t))$ is a reset value of the state $X_i(t)$. When the state $X_i(t)$ reaches the threshold $B(R_i(t))$, and the i th membrane-unit accepts the signal from the internal clock $CL_i(t)$ or the external stimulation input $s(t)$, the state $X_i(t)$ resets to $X_i(t) = A(P(t))$ and the model outputs a signal to the membrane threshold resistor. Depending on the output signal, the threshold

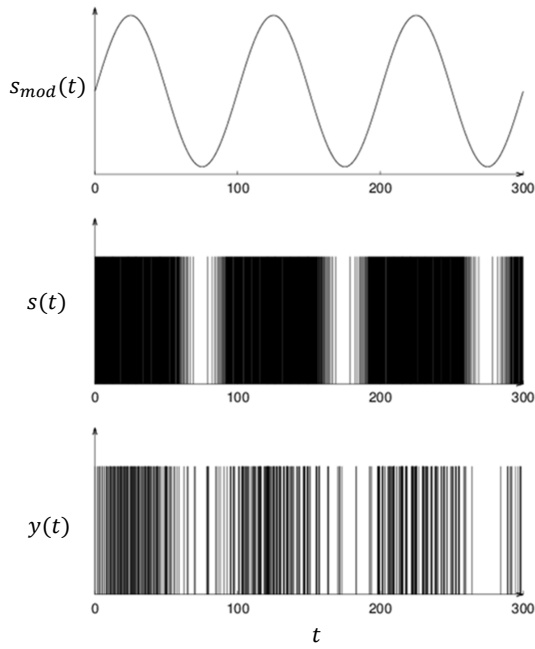


Figure 5: Input signal $s(t)$ and logical sum $y(t)$ of the whole outputs $y_i(t)$, $i = 0, \dots, N - 1$.

$B(R_i(t))$ increases. Repeating this dynamics, the threshold value of the state $X_i(t)$ increases. When the recovery threshold resistor and the membrane threshold resistor accept the signal from the external clock $Cu(t)$, the state $Q(t)$ and the state $R_i(t)$ decrease, and the threshold value of the state $P(t)$ and the state $X_i(t)$ decrease. Fig. 4(f) shows an output y_i of the i th membrane-unit. When the state $X_i(t)$ is at the threshold value (i.e., $X_i(t) = B(R_i(t))$ or $X_i(t) > B(R_i(t))$), the presented model outputs a spike $y_i(t) = 1$.

Fig. 5 shows an input signal $s_{mod}(t)$, a pulse density modulation $s(t)$ of the input signal $s_{mod}(t)$ and a logical sum $y(t)$ of the whole outputs $y_i(t)$, $i = 0, \dots, N - 1$. As shown in Figs. 5(c) and (d), it can be confirmed that the modulation signal $s_{mod}(t)$ is encoded into N paralleled spike-trains $(y_0(t), \dots, y_{N-1}(t))$, where the spike density of the logical sum $y(t)$ mimics the modulation signal $s_{mod}(t)$. Such a parallel encoding function can be found in the mammalian cochlear [1].

3.2. Adaptation property

We define an output spike-train's histogram $h(t)$ by the following equation:

$$h(t) = \text{Number of spikes in } y(t) \text{ for } mw \leq t < (m + 1)w,$$

where $m = 0, 1, 2, \dots$ and w is a bin width of the histogram. Fig. 6 shows a histogram of the logical sum $y(t)$ of the whole outputs $y_i(t)$. In this figure, the bin width is $w = 100$. It can be confirmed in this figure that the model

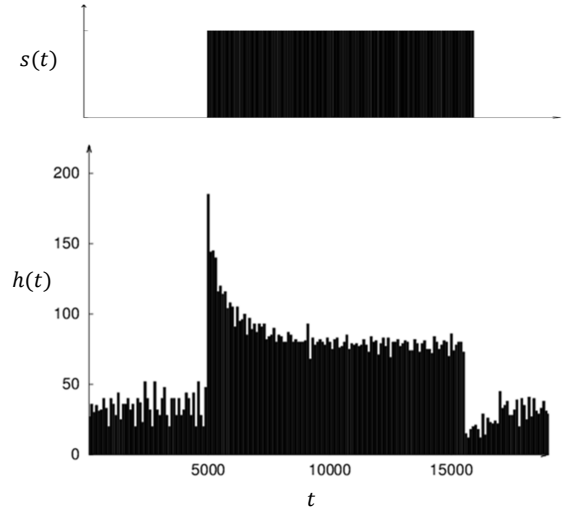


Figure 6: Histogram of the logical sum $y(t)$ of the whole outputs $y_i(t)$.

has an adaptation property, i.e., this model can detect the onset of the input spike-train $s(t)$. Such an adaptation property can be found in the mammalian cochlear [2].

4. Conclusions

We presented the spiral ganglion cell model by using the asynchronous cellular automaton. We showed that the model exhibits nonlinear properties found in the mammalian cochlear, i.e., the parallel encoding function and the adaptation property. Future problems are including following ones: (a) FPGA implementation and (b) more detailed analysis. The authors would like to thank Professor Toshimitsu Ushio of Osaka Univ. for valuable discussions. This work was partially supported by the support center for advanced telecommunications technology research (SCAT), the telecommunications advancement foundation (TAF), Toyota Riken Scholar, and KAKENHI Grant Number 24700225.

References

- [1] Geisler, C.D. From sound to synapse: physiology of the mammalian ear, Oxford University Press, (1997).
- [2] J. E. Rose, J. F. Brugge, D. J. Anderson and J. E. Hind, Phase-locked response to low-frequency tones in single auditory nerve fibers of the squirrel monkey, *J Neurophysiol*, vol. 30, pp. 769-793, (1967).
- [3] S. Hashimoto and H. Torikai, A novel hybrid spiking neuron: bifurcations, responses, and on-chip learning, *IEEE, Transactions on circuit and systems*, vol. 57, No. 8, pp. 2168-2181, (2010).
- [4] H. Torikai. and T. Nishigami, An artificial chaotic spiking neuron inspired by spiral ganglion cell: Paralleled spike encoding, theoretical analysis, and electronic circuit implementation, *Neural Networks*, Vol. 22, Issues 5-6, pp. 664-673, (2009).